Proc. Natl. Acad. Sci. USA
Vol. 86, pp. 7736–7740, October 1989
Biochemistry

Refined apoprotein structure of rat intestinal fatty acid binding protein produced in *Escherichia coli*

(protein structure/x-ray crystallography/fatty acid–protein interactions)

JAMES C. SACCHETTINI*, JEFFREY I. GORDON*‡, AND LEONARD J. BANASZAK*†

Departments of *Biochemistry and Molecular Biophysics and ‡Medicine, Washington University School of Medicine, Saint Louis, MO 63110

Communicated by Carl Frieden, July 13, 1989 (received for review April 20, 1989)

ABSTRACT **Rat intestinal fatty acid binding protein (I-FABP) is a member of a family of cytoplasmic hydrophobic ligand-binding proteins. To gain insights about the contribution of bound fatty acid to I-FABP's conformation and mechanism of ligand binding, we have determined the structure of *Escherichia coli*-derived rat apo-I-FABP to 1.96-Å resolution and compared it to the recently refined structure of I-FABP with bound palmitate. Both apo- and holo-I-FABP are composed primarily of anti-parallel β-strands which form two nearly orthogonal β-sheets ("β-clam"). The overall structures of the apo- and holo-I-FABP are nearly identical, with a root mean square (rms) difference of 0.37 Å between C^{α} atoms, 0.38 Å between all main-chain atoms, and 0.94 Å between all side-chain atoms. However, rms differences of greater than 1.3 Å were noted for the side chains of Ile-23, Lys-27, Arg-56, Leu-72, Ala-73, and Asp-74. The space occupied by bound ligand in the core of the holoprotein is occupied in the apoprotein by ordered solvent molecules. This results in an increase in the total number of internal ordered solvent molecules from 7 in the holoprotein to 13 in apo-I-FABP. This finding, together with observed differences in the side-chain orientations of two residues (Arg-56 and Lys-27) situated over a potential opening to the cores of the apo- and holoproteins, suggests that solvent molecules play a critical role in ligand binding. Moreover, the data indicate that the β-clam structure is stable even in the absence of bound ligand.**

Rat intestinal fatty acid binding protein (I-FABP) is a 15-kDa protein which binds one molecule of long-chain saturated or unsaturated fatty acid in a noncovalent manner with K_d values of 1–4 μM (1). Although the precise function of this cytoplasmic protein is not known, it is believed to participate in the uptake, intracellular targeting, and/or metabolic processing of fatty acids within the intestinal epithelial cell population (2). In addition, I-FABP may protect other proteins and membranes from the deleterious effects of high concentrations of fatty acids.

I-FABP is a member of a family of cytoplasmic hydrophobic ligand-binding proteins that contains 10 known members (summarized in refs. 3–5). The tertiary structures of I-FABP (6, 7) and the homologous P2 protein of peripheral nerve myelin (3) have recently been determined with bound fatty acid. Both holoproteins consist of two nearly orthogonal β-sheets formed by 10 antiparallel β-strands. This structure resembles a clam shell and has been called a "β-clam" (6). The C^{α} structures of I-FABP and P2 with bound ligand are remarkably similar (3, 7) with a calculated root-mean-square (rms) difference of less than 1.8 Å. The overall conformations of I-FABP and P2 resemble those of a group of *extracellular* hydrophobic ligand-binding proteins. This group includes serum retinol-binding protein (8), bilin-binding protein/insecticyanin (9–11), β-lactoglobulin (12–14), and several other sequences. All of these extracellular proteins have eight antiparallel β-strands forming a β-barrel that is open to the exterior at one end. The ligand-binding sites have been defined for several members of this superfamily of intra- and extracellular proteins (3, 7–14). All of these proteins have their bound ligands located within their cores. For P2 (3) and I-FABP (7), the fatty acids occupy a significant volume of this interior cavity. The interactions that occur between many of the internal amino acid side chains and the bound fatty acid appear to be important for maintaining the conformation of the ligand and possibly the protein itself. However, direct exploration of the latter notion has been "limited" to the use of molecular dynamic simulations. For example, Åqvist *et al.* (15) have used the coordinates of serum retinol-binding holoprotein to predict the tertiary structure of the corresponding apoprotein.

To directly examine the role of ligand in maintaining the conformation of a representative β-clam protein, we have determined the tertiary structure of apo-I-FABP at 1.96-Å resolution. A comparison of the refined structures of the apoprotein and the holoprotein (containing bound palmitate) indicates that the overall conformation of I-FABP does not change upon removal of ligand. Nonetheless, very distinct movements of several side chains located near a potential opening to the protein's core have been identified. Six more ordered solvent molecules were observed within the apoprotein's cavity in addition to the seven already present in the holoprotein. One of these appears to occupy a position within the apoprotein which is analogous to that of the carboxylate group of the bound palmitate present in holo-I-FABP. A hypothesis is presented that links solvent to ligand binding in this, and potentially other, hydrophobic ligand-binding proteins.

MATERIALS AND METHODS

Preparation of Crystalline Delipidated Rat I-FABP from *Escherichia coli*. Rat I-FABP was expressed and purified from *E. coli* (1, 7). The protein was then delipidated by passage through hydroxyalkoxypropyldextran (Lipidex 1000, Sigma), using a previously described protocol (1). The extent of delipidation was judged to be greater than 98% on the basis of a [^{14}C]palmitate-binding assay (1). Crystals of apo-I-FABP were produced by free interface diffusion (16) under conditions identical to those used to crystallize palmitate-complexed, *E. coli*-derived rat I-FABP (6, 7); i.e., the final solution contained I-FABP (20 mg/ml) piperazine-*N*,*N*'-bis(2-ethanesulfonic acid) (10 mM, pH 7.3), and polyethyleneglycol 4000 (Baker; 24%, wt/vol) in a Teflon-stoppered 2.0-ml glass vial (Wheaton Scientific). Precession photographs of these crystals revealed a monoclinic $P2_1$ space group with unit cell dimensions of a = 36.0 Å, b = 56.6 Å, c

The publication costs of this article were defrayed in part by page charge payment. This article must therefore be hereby marked "*advertisement*" in accordance with 18 U.S.C. §1734 solely to indicate this fact.

Abbreviation: I-FABP, intestinal fatty acid binding protein.

†Present address: Department of Biochemistry, University of Minnesota, 435 Delaware Street, Southeast, Minneapolis, MN 55455.

Table 1. Results of the rotation and translation functions obtained by using the MERLOT computer package

Probe	Holo-I-FABP; 1057 atoms
Apo-I-FABP data	7.0–3.5 Å, $I > 2\sigma$
Patterson radius	20.0 Å
Unit cell	$a = b = c = 90.0$ Å and $\alpha = \beta = \gamma = 90.0°$
Rotation function	$\alpha = 155°$, $\beta = 92°$, $\gamma = 270°$
Translation function	$TA = 0.30$, $TB = 0.50$, $TC = 0.52$ 6.3 rms units
R-factor minimization	$\alpha = 155.75$, $\beta = 90.66$, $\gamma = 271.29$ 12.0 rms units
Solution	$TA = 0.346$, $TB = 0.500$, $TC = 0.524$
R factor	30.4%

= 31.6 Å, and $\beta = 113.1°$. Each asymmetric unit contains one molecule of I-FABP.

Data Collection and Processing. X-ray diffraction data for crystalline apo-I-FABP were collected on a CAD4 diffractometer. Six crystals produced in a single vial were used for all of the data collection. Single I-FABP crystals were used to obtain data in shells of resolution. Each shell of data was overlapped with other resolution-range shells to allow for the collection of common reflections for scaling purposes. Lorentz-polarization and absorption corrections were done as described (7). Diffraction data were processed, scaled, and merged with the ROCKS X-ray crystallographic program package (17), yielding an *R*-merge on intensity of 14% for the complete data set. This relatively high *R* factor is probably due to errors for the reflections with low net intensities, including many of the high-resolution reflections. Specifically, the *R* factor for merging data between 10 Å and 2.5 Å was 8.2%, while the *R* factor for data between 2.5 Å and 2 Å was 16.2%.

X-Ray Phasing Method. The tertiary structure of crystalline apo-I-FABP was solved by using the molecular replacement method incorporated into the program package MERLOT (18). The refined model of palmitate-complexed I-FABP (7), without solvent and fatty acid, was used as a probe to solve the Crowther fast rotation function (CROSUM) as well as the translation function (TRANSUM) for the apoprotein. These results are presented in Table 1.

The values of α, β, and γ in the solution of the rotation function suggested that it was possible to reindex the apo-I-FABP data in the reciprocal lattice of holo-I-FABP. The transformation matrix used for this reindexing was

$$\begin{bmatrix} h \\ k \\ l \end{bmatrix}_{\text{holo}} = \begin{bmatrix} 1 & 0 & 1 \\ 0 & -1 & 0 \\ 0 & 0 & -1 \end{bmatrix} \times \begin{bmatrix} h \\ k \\ l \end{bmatrix}_{\text{apo}}$$

The resulting unit cell parameters after reindexing were a = 37.4 Å, b = 56.6 Å, c = 31.6 Å, and $\beta = 117.9°$. These values, when compared to the unit cell of holo-I-FABP (a = 36.8 Å, b = 56.9 Å, c = 31.9 Å, and $\beta = 114.0°$) indicate a slight change in the unit cell dimensions and a 4.9° change in the β angle. The *R* factor between the reindexed apo-I-FABP and the holo-I-FABP data from 15 Å to 3 Å was 32% (versus 56% for the mismatched indexing). The initial indexing scheme was used for the apo-I-FABP data.

Refinement of Apo-I-FABP to 1.96-Å Resolution. Energy refinement and molecular dynamics (19), least-squares refinement (20), and molecular model building were used to complete the high-resolution tertiary structure of apo-I-FABP. The refinement results are presented in Table 2. The results of the molecular replacement were applied to the model of holo-I-FABP, without solvent or fatty acid. This model was first refined with structure-factor-restrained energy refinement and molecular dynamics simulation by using XPLOR (19). The charged forms of aspartate, glutamate, histidine, arginine, and lysine were used in the energy refinement and subsequent molecular dynamics. No restraints were placed on C^α atoms to limit their movement. Sixty steps of energy refinement and a 1.25-ps molecular dynamics simulation (1-ps heat stage and 0.25-ps cool stage) reduced the *R* factor for 8- to 2.8-Å resolution data from 34.0% to 18.9%. A $|F_o| - |F_c|$ electron density map, displayed on an Iris (Silicon Graphics) workstation running the molecular model building software TOM, was then used to determine the position of solvent molecules. Thirty solvent molecules in the apoprotein were initially found to be within 2.0 Å of their original positions in the holoprotein. Twenty-five new solvent molecules were added to the model, which was used as the starting point for two iterations of least-squares positional and temperature factor refinement with TNT (20). TNT was run by first relaxing and then tightening the geometrical restraints on the model over a number of iterations (referred to as a macrocycle). This was followed by individual temperature factor refinement when data resolution was greater than 2.3 Å. Least-squares refinement provided a quick and convenient way to incorporate higher resolution phases and judge the assignment of solvent molecules. Ten solvent molecules with temperature factors greater than 50 Å^2 were removed from the model and seven new solvent molecules were added after TNT. No attempt was made to refine the occupancy of solvent.

Data from 7.0-Å to 1.96-Å resolution (5990 reflections with $|F_o| > 1.5\ \sigma$) were next used for structure factor restrained energy refinement and molecular dynamics simulation. This was performed in the same manner as the first phase of XPLOR described above, with the inclusion of higher-resolution data (see Table 2). The resultant model and two electron density maps ($|F_o| - |F_c|$ and $2|F_o| - |F_c|$) were used for a final rebuilding of the molecular model. The positions of all atoms and all significant difference electron density peaks were examined and corrected during this stage of the structure determination. A final macrocycle of TNT was run, allowing

Table 2. Comparison of crystallographic and molecular dynamics refinement results for apo-I-FABP

Measurement	Procedure			
	XPLOR	TNT	XPLOR	TNT
Resolution range, Å	8.0–2.8	7.0–1.96	7.0–1.96	7.0–1.96
No. of reflections	2886	5990	5990	5990
No. of solvent molecules		55	52	62
R factor,* %	18.9	19.3	20.3	18.8
rms bond length, Å	0.018	0.016	0.016	0.016
rms bond angle, °	4.04	3.18	3.54	2.93
rms torsional angle, °	30.41	31.18	30.24	30.31
Energy, arbitrary units	−1616	ND	−2805	ND

ND, not determined.
*The starting *R* factor is 34%.

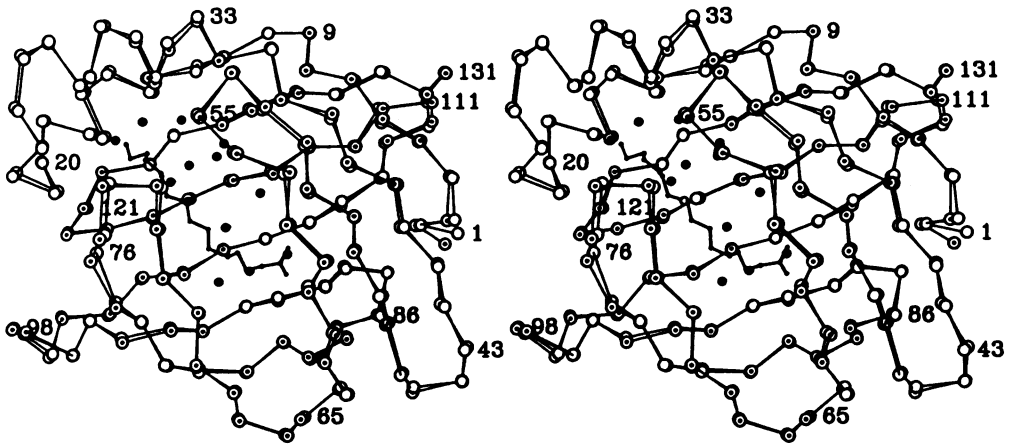

FIG. 1. Stereodiagrams showing the superimposition of the C^{α} coordinates of holo-I-FABP (○) and apo-I-FABP (○). The bound palmitate (16:0) in the holoprotein (7) can be seen within the core of the β-clam. The 13 ordered solvent molecules located within the core of apo-I-FABP are shown as ●.

us to refine the model to the geometry shown in Table 2 and to finalize the positions of the 62 ordered solvent molecules.

To verify the positions assigned to ordered solvent in the final model of apo-I-FABP, a macrocycle of TNT was run while using the final coordinates without solvent. The resultant $|F_o| - |F_c|$ electron density map showed that the set of solvent positions in the final model was consistent with the difference density in this "omit" map.

RESULTS AND DISCUSSION

Quality of the Refined Structure of Apo-I-FABP. The refined structure of apo-I-FABP had an *R* factor of 18.5% when data from 7.0- to 1.96-Å resolution with intensities greater than 1.5 σ (5990 reflections out of 8550 possible reflections or 70%) were used. A Luzzati plot of the *R*-factor for these data versus different mean positional errors indicates an rms error in atomic coordinates of 0.23 Å. The rms deviations of the bond lengths and bond angles from ideality for the final model were 0.016 Å and 2.93°, respectively. The φ and ψ angles for the refined structure fall within the allowed areas of a Ramachandran plot (data not shown). A $|F_o| - |F_c|$ electron density map calculated with the refined apo-I-FABP structure had no positive or negative density peaks greater than 3 σ. This difference map when contoured at 1.5 σ did not show any continuous positive electron density which could be interpreted as a bound fatty acid. The structure contained no solvent molecules with temperature factors greater than 50 $Å^2$. In addition, there were no assigned solvent atoms with very low temperature factors (i.e., 1–3 $Å^2$), indicating that the solvent atom in question was possibly an ion.

Holo- and Apo-I-FABP Have Similar Overall Structures. We have recently determined the high-resolution tertiary structure of I-FABP containing bound palmitate (7). The protein contains 10 antiparallel β-strands (named βA–βJ) arranged in two nearly orthogonal β-sheets (Fig. 1). Two α-helices are located between βA and βB. Helix I appears as a continuation of the first β-strand (A) and is connected to helix II via a sharp turn. Helix II is continuous with strand βB.

Holo-I-FABP has a relatively large surface area containing many charged side chains. A 9-Å "gap" is present between the C^{α} chains of βD and βE (residues 55–73 in Fig. 1). In the holoprotein, this "gap" is bridged by the side chains of amino acids contained in these two strands and by ordered solvent molecules (7). Fifty-three bound solvent molecules were identified on the surface of the holoprotein, forming a fairly uniform solvent surface. A solvent-accessible opening ("portal") to the core of the protein is formed by the tight turns which occur between β-strands C and D, E and F, and helix αII (residues 24–33 in Fig. 1). This area was thought to be a potential entry and/or exit site for the fatty acid (7).

The *overall* structure of apo-I-FABP is nearly identical to that of the palmitate-containing protein described above (see Figs. 1 and 3). Superimposition of the two structures yields a calculated rms deviation of 0.37 Å for C^{α} atoms (Fig. 1), 0.38 Å for all main-chain atoms, and 0.94 Å for all side-chain atoms. Like that of the holoprotein, the surface of apo-I-FABP is made up of the side chains of many ionizable amino acids (Fig. 2) and bound solvent molecules. We have refined the positions of 62 ordered solvent molecules in the apoprotein. Thirty-five of these solvent molecules are located within 2.0 Å of the positions occupied by solvent molecules in the superimposed holoprotein. There are no gross conformational differences in the main chains of the two proteins which could result in a large change in the surface charge. This was confirmed by superimposition of the two models, in which no obvious variation in the surface charge distribution could be

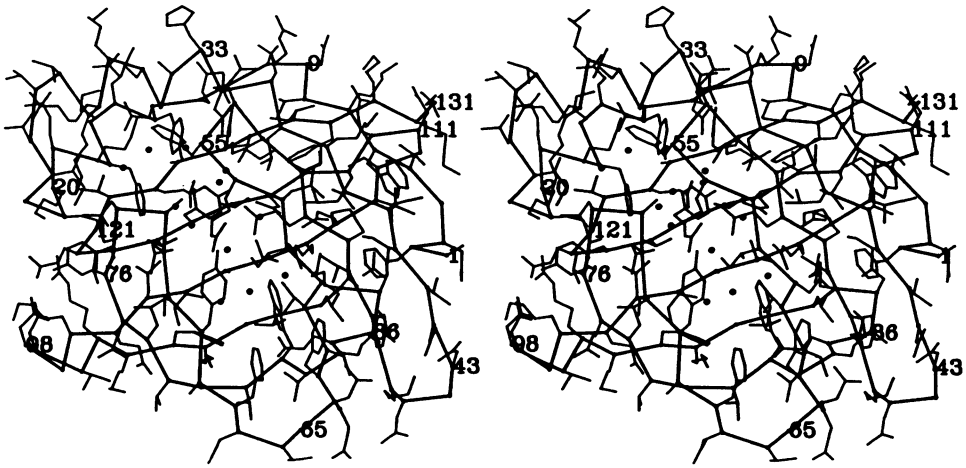

FIG. 2. Stereodiagram of the refined molecular structure of apo-I-FABP showing location of side chains and ordered internalized solvent. Internalized ordered solvent molecules are represented by ●.

detected, although close inspection of the two structures did reveal a number of minor differences in the orientations of exterior side chains.

Differences Between the Structures of Holo- and Apo-I-FABP. The largest variation between the C^{α} positions of the two models occurs in the first three NH_2-terminal residues (Fig. 1). These differences may be attributable to flexibility normally found for NH_2-terminal regions of proteins. There are also a number of side-chain differences, which are principally located within the so-called portal region of the proteins. Of particular interest is the position of the side chains of Arg-56 and Lys-27 (see Fig. 3 *Upper*). In the holoprotein, the guanidinium group of Arg-56 points towards β-strand E, leaving one of its amino groups oriented towards the exterior and the other towards the interior of the protein. The exteriorly oriented amino group is hydrogen bonded to an ordered solvent molecule and the other amino group is part of an internal "electrostatic network" including two solvent molecules, Tyr-70, and Glu-51. By contrast, the entire guanidinium group of Arg-56 is tucked into the interior of apo-I-FABP, forming a number of hydrogen bonds with internal solvent and Tyr-70, Glu-51, and Ser-71. In the apoprotein, the side chain of Lys-27 spans this potential opening, closing off the core to the surface, while in the holoprotein the side chain of Lys-27 is in a position that allows access of exterior solvent to the core. As discussed below, these side chains may affect solvent movement to and from the interior of I-FABP.

The Fatty Acid Binding Site Is Occupied by Ordered Solvent Molecules in Apo-I-FABP. The refined 2.0-Å structure of I-FABP with bound palmitate indicated that a single molecule of fatty acid was present in the interior of the β-clam (7). Its carboxylate group is buried deep in the protein, while the bent hydrocarbon tail extends toward the portal parallel, and in close proximity, to strands βD and βE (Fig. 1). The carboxylate group was hydrogen bonded to the guanidinium group of Arg-106 via an electrostatic network containing at least three other polar groups: the side-chain oxygen of Asn-115 and two ordered solvent molecules.

The core of I-FABP with bound palmitate also contains seven ordered solvent molecules. These solvent molecules are distributed along the length of the concave face of the bent fatty acid, close to the "gap" between β-strands D and E.

The interior cores of apo- and holo-I-FABP are remarkably similar. No significant side-chain movement can be detected for most of the amino acids, including those which interact with the fatty acid in the holoprotein. Fifteen amino acids in holo-I-FABP have atoms located within 4.1 Å of the bound palmitate (Tyr-14, Phe-17, Met-18, Ile-23, Lys-27, Phe-55, Val-60, Tyr-70, Leu-72, Ala-73, Asp-74, Trp-82, Phe-93, Arg-106, and Tyr-117). The positions of the side-chain atoms of these residues in the apoprotein show an overall rms difference

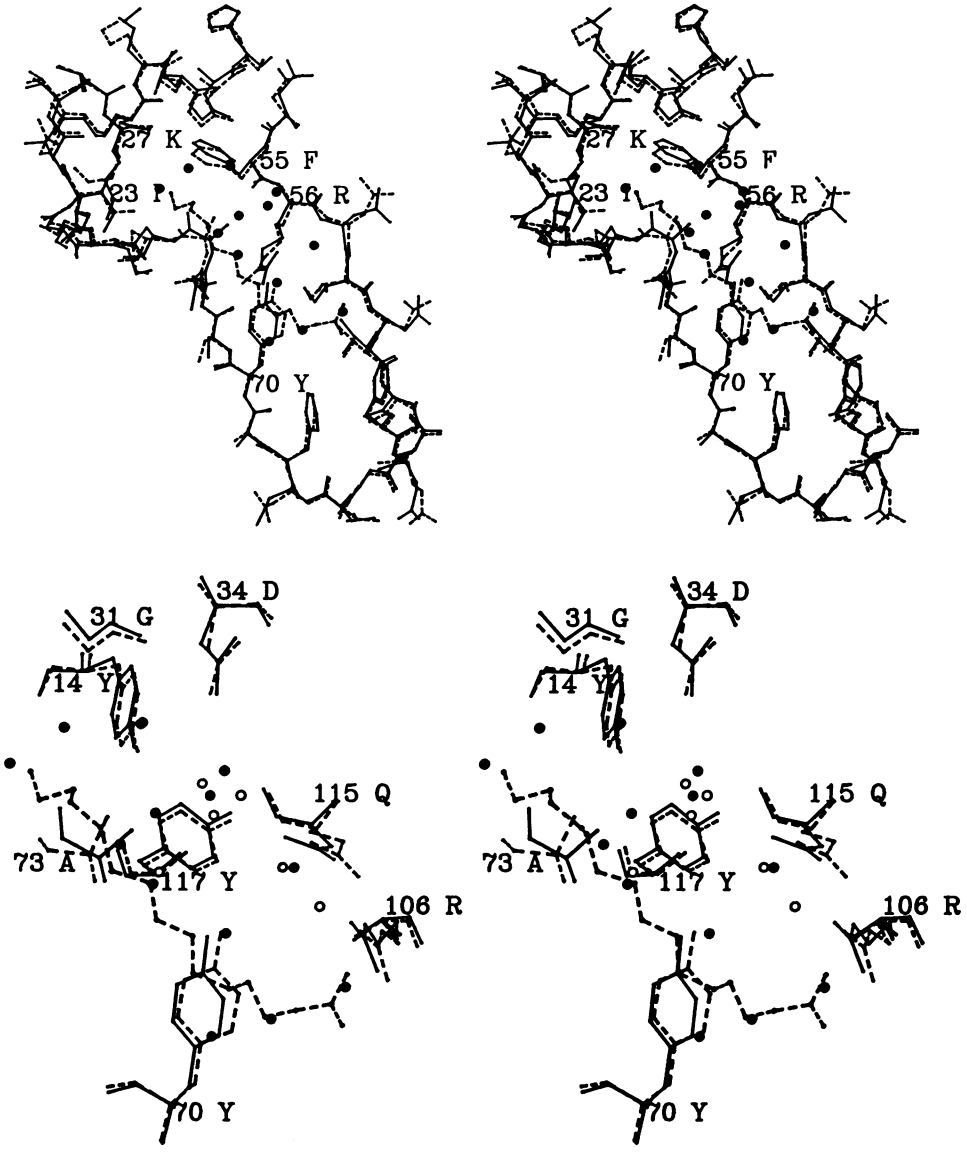

FIG. 3. Stereodiagrams of selected regions of apo- and holo-I-FABP. (*Upper*) Superimposition of the two proteins in the region of a solvent-accessible opening to their cores. (*Lower*) Superimposition of the two proteins in the region of the ligand-binding site. The broken lines represent bonds between atoms of the holoprotein, while solid lines denote such bonds in apo-I-FABP. In both panels, solvent molecules of apo-I-FABP are represented by ●.

of 0.78 Å. Of these, only Ala-73 shows any significant main-chain movement (rms = 1.5 Å). Moreover, most of the conformational dissimilarity is restricted to the side chains of Ile-23, Lys-27, Leu-72, Ala-73, and Asp-74. The rms difference for the side chains of these residues is 1.4 Å. The side chains of Ile-23, Leu-72, and Ala-73 are oriented in the direction of the bound fatty acid in holo-I-FABP. In the apoprotein, they are directed toward other hydrophobic regions. For example, in the holoprotein, the δ-carbon of Ile-23 is pointing toward, and is within van der Waals radius of, the C16 atom of the bound palmitate. However, in the refined structure of the apoprotein, the C^{δ} of Ile-23 is turned away and points toward the interior of the protein (Fig. 3 *Upper*).

While the side chains of residues which appear to provide critical interactions with the bound ligand are comparably positioned within the cores of the apo- and holoproteins (e.g., note the superimpositions of Tyr-70, Arg-106, and Gln-115 in Fig. 3 *Lower*), significant differences were noted in numbers and locations of ordered solvent molecules. The interior of the apoprotein contains 13 ordered solvent molecules; 6 are located in positions which are occupied by comparable solvent molecules in the holoprotein, while additional solvent molecules are present at locations which are close to those occupied by the C1, C2, C8, and C15 atoms of palmitate (Figs. 1 and 3). An ordered solvent molecule replaces the carboxylate group of palmitate, permitting the apoprotein to retain the five-membered hydrogen bonding network analogous to that present in the holoprotein. Thus, in the apoprotein, this complex consists of three, rather than two, ordered solvent molecules as well as the side-chain oxygen of Gln-115 and the δ guanidinium group of Arg-106. There is no continuity of electron density in either the $2|F_o| - |F_c|$ map or the $|F_o| - |F_c|$ map of apo-I-FABP which could be construed as bound fatty acid. Moreover, the refined temperature factors of the ordered solvent atoms in this area are consistent with the idea that they represent ordered solvent and are not density from other molecules such as buffer ions. Furthermore, a significant volume of the core of apo-I-FABP is not occupied by ordered atoms.

Proposed Mechanism of Fatty Acid Binding. In the high-resolution study of holo-I-FABP (7), we proposed that the entry of palmitate into the interior of the protein may be facilitated by a series of charge interactions occurring between its carboxylate group and a number of polar side chains. Binding of the carboxylate group to the side chain of a basic amino acid located on the surface of the protein would be followed by ligand entry through the portal area and subsequent incorporation of the carboxylate into the five-membered hydrogen bonding network. In this scheme, the conformation assumed by the hydrocarbon tail would be dictated by the hydrophobic binding pocket formed by the side chains of nonpolar and aromatic amino acids, although it was not clear to what extent the ligand affected the location of these side chains. This pathway would allow the protein to incorporate the fatty acid without distorting its native conformation (i.e., by breaking many hydrogen bonds or moving a number of hydrophobic side chains). Our analysis of the structure of apo-I-FABP is consistent with this type of mechanism. Specifically, it now appears that the final conformational state of crystalline apo-I-FABP is remarkably similar to that of the protein with bound ligand. This suggests that the β-clam structure is not dependent upon the presence of bound fatty acid. Moreover, the data indicate that ligand removal is associated with little alteration in the orientation of side chains in the portions of the binding pocket which interact with either its carboxylate group or its hydrocarbon tail. At least two observations suggest that ordered solvent molecules may play a role in the process of ligand acquisition and removal: (*i*) six "extra" ordered solvent molecules occupy the protein core in areas previously populated by ligand, and (*ii*) some of the most "dramatic" differences in the side chain orientations of apo- and holo-protein can be mapped to those residues which overlie a potential opening to their cores. One testable hypothesis arising from these structural studies is that acquisition and release of fatty acids by I-FABP is intimately related to a subtle low-energy process predicated on solvent movement. Moreover, such movement may be affected in part by the mobile side chains of Arg-56 and/or Lys-27. In this scheme, the presence of more ordered solvent molecules in the interior of the apoprotein compared to the holoprotein could be an entropic factor which favors fatty acid binding. Additional higher resolution studies of apo- and holo-I-FABP are needed to better define the nature and interactions of ordered solvent. Site-directed mutagenesis of I-FABP and subsequent expression of genetically engineered protein(s) in *E. coli* should also provide a way of directly examining the hypothesis that alterations in solvent movement play an important role in the binding mechanism.

This work was supported by grants from the National Institutes of Health (GM13925 and DK30292) and Monsanto. J.C.S. is the recipient of a postdoctoral fellowship from the American Heart Association, Missouri Affiliate. J.I.G. is an Established Investigator of the American Heart Association.

1. Lowe, J. B., Sacchettini, J. C., Laposata, M., McQuillan, J. J. & Gordon, J. I. (1987) *J. Biol. Chem.* **262,** 5931–5937.
2. Sweetser, D. A., Heuckeroth, R. O. & Gordon, J. I. (1987) *Annu. Rev. Nutr.* **7,** 337–359.
3. Jones, T. A., Bergfors, T., Sedzik, J. & Unge, T. (1988) *EMBO J.* **7,** 1597–1604.
4. Bohmer, F.-D., Kraft, R., Otto, A., Wernstedt, C., Hellman, U., Kurtz, A., Muller, T., Rohde, K., Etzold, G., Lehmann, W., Langen, P., Heldin, C.-H. & Grosse, R. (1987) *J. Biol. Chem.* **262,** 15137–15143.
5. Walz, D. A., Wider, M. D., Snow, J. W., Dass, C. & Desiderio, D. M. (1988) *J. Biol. Chem.* **263,** 14189–14195.
6. Sacchettini, J. C., Gordon, J. I. & Banaszak, L. J. (1988) *J. Biol. Chem.* **263,** 5815–5819.
7. Sacchettini, J. C., Gordon, J. I. & Banaszak, L. J. (1989) *J. Mol. Biol.* **208,** 327–339.
8. Newcomer, M. E., Jones, T. A., Aqvist, J., Sundelin, J., Eriksson, U., Rask, L. & Peterson, P. A. (1984) *EMBO J.* **3,** 1451–1454.
9. Holden, H. M., Rypniewski, W. R., Law, J. H. & Rayment, I. (1987) *EMBO J.* **6,** 1565–1570.
10. Huber, R., Schneider, M., Epp, O., Mayr, I., Messerschmidt, A., Pflugrath, J. & Kayser, H. (1987) *J. Mol. Biol.* **195,** 423–434.
11. Huber, R., Schneider, M., Mayr, I., Muller, R., Deutzmann, R., Suter, F., Zuber, H., Falk, H. & Kayser, H. (1987) *J. Mol. Biol.* **198,** 499–515.
12. Sawyer, L., Papiz, M. Z., North, A. C. T. & Eliopoulos, E. E. (1985) *Biochem. Soc. Trans.* **13,** 265–266.
13. Papiz, M. Z., Sawyer, L., Eliopoulos, E. E., North, A. C. T., Findley, J. B. C., Sivaprasadaro, R., Jones, T. A., Newcomer, M. E. & Kraulis, P. J. (1986) *Nature (London)* **324,** 383–385.
14. Monaco, H. L., Zanotti, G., Spadon, P., Bolognesi, M., Sawyer, L. & Eliopoulos, E. E. (1987) *J. Mol. Biol.* **197,** 695–706.
15. Åqvist, J., Sandblom, P., Jones, T. A., Newcomer, M. E., van-Gunsteren, W. F. & Tapia, O. (1986) *J. Mol. Biol.* **192,** 593–604.
16. Salemme, F. R. (1985) *Methods Enzymol.* **114,** 140–141.
17. Reeke, G. N., Jr. (1984) *J. Appl. Crystallogr.* **17,** 125–130.
18. Fitzgerald, P. M. D. (1988) *J. Appl. Crystallogr.* **21,** 273–278.
19. Brunger, A. T., Kuriyan, J. & Karplus, M. (1987) *Science* **223,** 458–460.
20. Tronrud, D. E., Ten Eyck, L. F. & Mathews, B. W. (1988) *Acta Crystallogr., Sect. A* **43,** 489–501.